Semiconductor Physics, Quantum Electronics & Optoelectronics, 2009. V. 12, N 2. P. 165-169.

PACS 78.47.Cd, 78.55.-m, 78.67.Bf, 81.15.Fg

Photoluminescent properties of Al_2O_3 films containing gold nanoparticles, which are prepared by pulse laser deposition

E.B. Kaganovich, I.M. Kizyak, A.A. Kudryavtsev, E.G. Manoilov
V. Lashkaryov Institute of Semiconductor Physics, NAS of Ukraine
41, prospect Nauky, 03028 Kyiv, Ukraine
E -mail: dept_5@isp.kiev.ua

Abstract. Photoluminescent porous films of aluminum oxide containing gold nanoparticles were prepared using pulse laser deposition from backward flow of particles from erosion torch. Measurements of time-resolved photoluminescence spectra revealed high intense photoluminescent band with the peak close to 2.4 eV and its low-energy shoulder at 1.6 - 1.7 eV, high-energy shoulder at 2.9 eV, with relaxation times up to several microseconds. Studied were the influence of formation conditions and gold concentrations in the target on photoluminescent properties of films. The nature of photoluminescence related with radiative recombination of electrons and holes in Au nanoparticles as well as local centers in Al_2O_3 matrix is discussed.

Keywords: aluminum oxide film, gold nanoparticles, time-resolved photoluminescence.

Manuscript received 03.02.09; accepted for publication 18.03.09; published online 20.03.09.

1. Introduction

Metal nanoparticles (NP) embedded into dielectric matrixes demonstrate new optical, photoluminescent, mechanical, thermal and other properties that are necessary to improve available device structures as well as develop some new ones. Optically excited metal surfaces possess either very weak or no photoluminescence (PL) at all. For the first time, in 1969 A. Mooradian [1] observed PL at the wavelength $\lambda = 520$ nm with the quantum efficiency 10^{-10} in plain films of bulk gold. Over a long period, they could not increase the PL intensity even in rough gold films [2]. But the situation was abruptly changed in the late 90s of the 20th and at the beginning of the 21st century when gold nanoparticles became the object of investigations [3-12]. The PL quantum efficiency grew by five – six orders in its magnitude in Au nanocolumns and nanoclusters with dimensions less than 15 nm [3, 4]. Positions of PL peaks comprised a wide range of wavelengths from the visible up to near infra-red part of the spectrum [2, 3, 5, 7].

The study of PL inherent to noble metals began from the above work by Mooradian [1]. The nature of gold PL was related with radiative recombination of electrons in 6sp conductive band and holes in 5d band. In the phenomenological model for PL that was offered by Boyd et al. [2], this radiative recombination was enhanced by local fields related with surface plasmons in gold. In Refs [5, 10], PL was explained with account of the processes when the excited holes of the 5*d*-band and 6*sp*-electrons recombinated nonradiatively with emission of surface plasmons that radiated later. The mechanisms of PL in Au NP are now under discussion. There considered are the possibilities to increase the efficiency of radiative recombination in semiconductor quantum dots and fluorescence of organic dye molecules due to local surface plasmons in Au NP [9]. Also considered are the processes of luminescence excitation in Au NP, in particular, the three-photon ones [9, 11].

Photoluminescent properties are inherent to various gold nanostructures prepared by different methods. These are island gold films obtained by nanostructuring [5]; Au:oxide composite multilayer systems where Au NP are located between oxides SiO_2, ZnO, TiO_2, deposited with magnetron sputtering [8]; suspensions of Au NP in methanol, water, prepared by laser ablation [9, 10]; Au NP in glass films formed by sol-gel technology [11], *etc*. To prepare photoluminescent composite films with Au NP, the method of pulse laser deposition (PLD) was used very seldom. However, this method can be related to developed technologies of

obtaining these composite structures. It possesses many advantages, namely: provides congruency of film composition, flexibility in controlling the parameters of deposition, which allows to control the matrix content, sizes, shape and concentration of nanoparticles [13]. Among various dielectric matrixes, where Au NP can be embedded, aluminum oxide is one of the most suitable due to the wide bandgap (9 eV) and high dielectric constant (close to 9), thermal stability, *etc*.

Recently in [12] obtained were photoluminescent films of amorphous Al_2O_3 containing Au nanocrystals with dimensions 5 nm. There used was the PLD method when deposition was realized using forward flow from erosion torch and following annealing in nitrogen atmosphere at 400 °C for 60 s. The authors observed the peak at 610 nm with the shoulder at 510 nm in the spectrum of stationary photoluminescence. The authors [12] excluded participation of local defects in this PL and suggested its relation with electron transitions in the vicinity of L- and X-points in the Brillouin zone of gold. To our knowledge, the possibilities to form photoluminescent films of Al_2O_3 with Au NP by using the PLD method with backward flow of torch particles and without following treatments remain indefinite. Also, not ascertained is the influence of the Au NP concentration and their sizes on photoluminescent properties of these films, their PL relaxation times, *etc*.

The aim of this work is to prepare photoluminescent Al_2O_3 films with Au NP by using the method of PLD from backward flow of erosion torch particles in one stage, to investigate their time-resolved PL spectra and study the influence of formation conditions on photoluminescent properties of these films.

2. Experimental

Thin rough gold films were prepared using the PLD method with forward high-energy flow of erosion torch particles, and composite films consisting of Au NP in Al_2O_3 dielectric matrix were obtained from backward low-energy flow of particles. We used silicon and silica substrates. YAG:Nd^{3+} laser beam (wavelength 1.06 μm, pulse energy 0.2 J, pulse duration 10 ns and repetition frequency 25 Hz) scanned the target in a vacuum chamber containing argon or oxygen with the pressure 5 to 20 Pa. When forming the gold films from forward particle flow, the substrate was placed in perpendicular to the torch axis at the distance 20 – 25 mm from the Au target. While forming the composite films, the substrate was placed in the plane of the target containing pieces of gold and aluminum.

The volume fraction of gold in the target (C_{Au}) was varied from 0 to 100 %. The density of irradiation energy was changed within the range $j = 5 – 20$ J/cm^2. Some films were thermally treated in air at temperatures 400 to 800 ºC for 10 to 30 min.

As a result of laser irradiation, created from the target is plasma consisting of atoms, ions and clusters of target material. Further adiabatic expansion of this plasma in the form of erosion torch results in interaction of torch particles with atoms of operation gas and respective dissipation of their energy. Energy losses are lower when depositing from forward particle flow, and higher during deposition from backward particle flow, when braking and flyback of particles to the substrate take place. In the latter case, one can observe separation of Au NP by their sizes: larger particles are deposited closer to the torch axis, and the smaller ones – farther. Thicknesses of films were in the range 5 to 500 nm. When films were prepared on the substrate placed in the plane of the target, the thickness profile was wedge-like.

Using the method of scanning atomic-force microscopy in the tapping mode, we ascertained that the surface of gold films deposited from forward particle flow is rough, the size of grains lies within the range up to 100 nm, size distribution of grains is rather wide. While the surface of films deposited from backward flow is smoother, but one can observed a lot of pores. The method of transmission electron microscopy of high resolution showed that the grain sizes were 10 to 20 nm in this case. As it follows from data of X-ray phase analysis, there exist amorphous phase of aluminum oxide as well as amorphous and cubic phases of gold.

Time-resolved PL spectra were measured in the energy range 1.4 – 3.2 eV using for excitation a nitrogen laser (wavelength 337 nm, pulse duration 8 ns) with stroboscopic signal registration in the photon counting mode. The strobe width was 250 ns.

3. Results and discussion

Studying the amorphous Al_2O_3 films deposited using backward flow of particles from erosion torch in argon, oxygen atmosphere, we observed PL with a low intensity (I_{PL}) and relaxation times (τ) shorter than 250 ns (Fig. 1). These PL spectra are wide, lie within the energy range 1.4 – 3.2 eV, position of their peaks is located near 2.5 – 2.8 eV. After annealing in air at 400 °C for 10 to 30 min, the PL spectra changed insignificantly, which confirms that radiative centers are retained in Al_2O_3. Moreover, it was impossible to anneal them at 800 °C for 30 min.

α-Al_2O_3 crystals with anion defects proved to be efficient luminophors. These crystals contain a relatively high concentration of oxygen vacancies V_O that provides capture centers for electrons, like to F-centers in alkali-halide crystals. Luminescent properties of α-Al_2O_3 crystals with anion defects are provided by aggregates of defects containing oxygen vacancies and impurity ions of transition metals, mainly titan and chromium. Here, the main emission centers are F-centers created by V_O defect capturing two electrons, with the emission peak at $\lambda \sim 410$ nm.

Photoluminescent properties of crystals and nanostructured α-Al_2O_3 are very similar [14-16]. When measuring the spectra of PL and cathodoluminescence for pressed powders and Al_2O_3 single crystals in

comparable conditions, the authors revealed the same characteristic emission bands for centers created by oxygen vacancies [14]. The PL spectrum of nanoporous anodized Al_2O_3 contained the intense wide band within the range 350–650 nm with its peak at 461 nm and an extended longwave wing. Approximation of this spectrum by Gaussians resulted in three bands with their peaks at 382 nm (3.2 eV), 461 nm (2.7 eV) and 500 nm (2.5 eV). These were related with F^+-, F- and F^{++}-centers [15], respectively. In composite films of amorphous Al_2O_3 with Si nanocrystals, they observed PL spectra with peaks at 415 nm caused by F-centers, and at 500 nm – by aggregate defects like to F_2-centers with various charge states [16].

In accord with the data of X-ray phase analysis, the prepared by us amorphous Al_2O_3 films possess a set of various non-equilibrium phases, have non-stoichiometric composition, and anion sub-lattice depleted by oxygen. Taking into account this fact along with known literature data, we related PL in the prepared films with emission of electron centers caused by F-centers and their aggregates of F_2 type. To our knowledge, data about PL relaxation times in Al_2O_3 films are absent. In this work, we ascertained that PL relaxation times for electron V_O-centers in these films are shorter than 250 ns. As it was mentioned in [14], if the time constant for F-center emission (3.0 eV) decay in α-Al_2O_3 crystals corresponds to a millisecond range, then all the emission bands of pulse cathodoluminescence in nanoceramic samples possess shorter times of the order of hundred nanoseconds. In the case of bands peaking at 3.0 and 3.4 eV, duration of emission decreased with decreasing the mean sizes of Al_2O_3 NP. It was impossible to anneal oxygen vacancies under thermal treatment in air at 400 ºC for 30 min. As was shown in [14], oxygen vacancies remain in Al_2O_3 powder after annealing in air at the temperature 500 ºC.

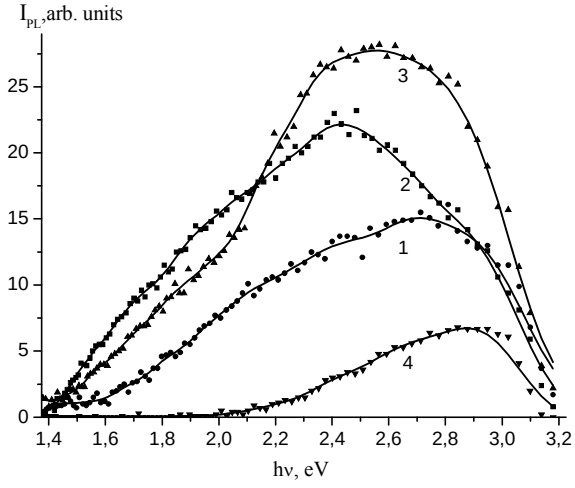

Fig. 1. PL spectra of Al_2O_3 films prepared in oxygen atmosphere at the pressure P = 6.5 Pa and the energy density of target irradiation j = 20 J/cm^2: as-deposited (*1*), annealed at 400 °C for 5 (*2*) and 30 min (*3*) as well as at 800 °C for 30 min (*4*). τ < 250 ns.

PL was not observed in thin gold films prepared using both forward and backward flows of particles from erosion torch. This fact agrees well with known data upon the very low intensity of PL that usually cannot be measured, which can be explained by radiationless energy relaxation related with Coulomb electron-electron scattering. The latter process is much faster than the radiative recombination of electron-hole pairs.

Just contrary, we observed intense PL when introducing Au NP into Al_2O_3 films. Starting from several percents of gold concentration in the target, the PL intensity and relaxation times increased abruptly (Fig. 2). As seen from comparison of Figs 1 and 2, the shape of PL spectra was changed, too. Multimodality of bands was clearly pronounced, and the intensity of low-energy shoulders was enhanced within the range of energies 1.4 – 1.8 eV. As a rule, the spectral peaks lay within the range 2.2 – 2.4 eV.

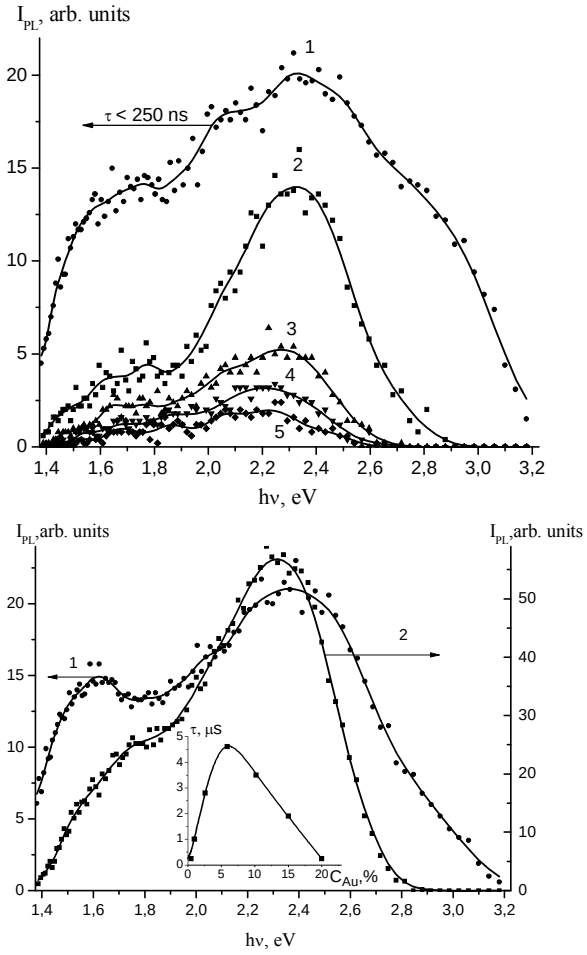

Fig. 2. Time-resolved PL spectra of Al_2O_3 films with Au NP prepared at the pressure P_{Ar} = 13.5 Pa and the energy density j = 20 J/cm^2, which differ by the gold concentration in the target C_{Au} and PL relaxation time τ:
a − C_{Au} = 1 %, (*1*) τ < 250 ns, (*2*) 250 < τ < 500 ns, (*3*) 500 < τ < 750 ns, (*4*) 750 ns< τ < 1 μs, (*5*) 1 < τ < 1.25 μs;
b − C_{Au} = 5 %, (*1*) τ < 250 ns, (*2*) 250 ns < τ < 4.5 μs.
Shown in the inset is the dependence of integrated PL relaxation time on the gold concentration in the target.

Shown in Fig. 2a are the time-resolved spectra for one of Al_2O_3 film with Au NP prepared taking C_{Au} = 1 % and j = 20 J/cm^2. Our analysis of the PL kinetics shows that if there exists the high-energy shoulder (2.9 eV) in the range of relaxation times $0 < \tau < 250$ ns, then with increasing the relaxation time up to 500 ns the intensity of this shoulder is sharply lowered, and at τ = 750 ns radiation with the energy 2.6 eV vanishes at all. If within the time range $0 < \tau < 250$ ns the intensity of the low-energy shoulder with the peak at 1.6 – 1.8 eV is high, then with increasing the relaxation time up to 500 ns its intensity sharply drops. During further PL relaxation, there remains the only band at 2.2 – 2.4 eV with the low-intense shoulder at 1.7 eV.

Juxtaposition of PL spectra inherent to Al_2O_3 films that do not contain gold with those obtained using introduction of gold into the target (see Figs 1 and 2) shows that for the former ones both the most intense peak and its shoulder are blue-shifted (up to 2.6 -2.7 eV and 1.8 – 2.0 eV, respectively), while for the latter ones (containing Au NP) these peak and its shoulder are, as a rule, red-shifted (down to 2.4 and 1.7 eV). One difference more: in the Al_2O_3 films without gold the PL relaxation times are less than 250 ns and the PL intensity is low, while in the same films with Au NP these relaxation times can lie in the microsecond range and the PL intensity is high. In the Al_2O_3 films containing Au NP, one can observe a correlated change in the intensity and PL relaxation times that are mainly determined by the radiationless recombination component. In this case, the quantum efficiency of PL does not exceed several percents.

Dependences of the PL intensity and relaxation time on the gold concentration in the target are non-monotonic (Fig. 2). When C_{Au} is less than 1 %, the τ value is doubly increased: from approximately 250 ns up to that reaching practically 500 ns. As the C_{Au} value grows from 1 – 2 up to 5 – 6 %, I_{PL} and τ values increase, τ reaches 5 – 6 μs. The further increase in C_{Au} value within the range 6 to 15 % results in decreasing values of I_{PL} and τ, when C_{Au} = 10 % τ is close to 3 – 4 μs, and for C_{Au} = 15-20 % the τ value does not exceed 250 ns (see inset in Fig. 2b). When the samples prepared at C_{Au} = 20 % were annealed for 10 min at the temperature 400 °C, the intensity of low-energy component in the PL band was decreased, while the PL relaxation time grew a little ($250 < \tau < 500$ ns). If the annealing temperature was increased up to 800 °C, PL vanished. It could not be also observed at C_{Au} = 75 % and j = 20 J/cm^2.

In Al_2O_3 films with gold nanoparticles, PL depends on the mode of target irradiation. *E.g.*, when C_{Au} equals to several percents and the density of irradiation energy is decreased from 20 down to 5 J/cm^2, τ values are shorten from 5 -6 μs down to 250 ns.

Our analysis of the influence of the target irradiation energy density on the PL intensity shows that the latter is high at j = 20 J/cm^2 when C_{Au} does not exceed 15 – 20 %, while at j = 5 J/cm^2 it is low already when C_{Au} reaches several percents. If at j = 20 J/cm^2 PL was not observed for $C_{Au} > 75$ %, then at j = 5 J/cm^2 it disappeared already for $C_{Au} > 20$ %.

The above results are indicative of the fact that PL is considerably determined by sizes of Au NP in these films Al_2O_3. But there exists an optimal dimension of nanoparticles, which corresponds to the highest intensity values and PL relaxation times. On the one hand, it is confirmed by the data of a monotonic growth in Au NP sizes with increasing the gold concentration in the target and irradiation energy density, and, on the other hand, by the observed non-monotonic dependences of these PL parameters on the above technological conditions.

Thus, the PL spectra observed in Al_2O_3 films with Au NP possess features related both with local defects in the matrix itself (high-energy fast components) and with Au NP and their sizes (low-energy slow components). To find PL mechanisms in these films needs further investigations. Respective PL models can be related with interband transitions in gold (1.8 and 2.4 eV), with enhanced radiative recombination near Au NP due to local electric fields caused by local surface plasmons, with emission of these plasmons themselves, and, finally, with transfer of excited carriers between local centers related to defects in Al_2O_3 and Au NP, as well as between Au nanoparticles of various sizes.

Preliminary investigations aimed at optical properties of Al_2O_3 films with Au NP allowed to find that the resonant absorption band caused by local surface plasmons is inherent, as a rule, to rough gold films as well as to Al_2O_3 films with Au NP prepared with high gold concentration in the target (C_{Au} = 20 – 75 % and j = 20 J/cm^2), i.e., in the samples with very weak PL or in those without any PL. Our preliminary results indicate that the used conditions to form these films do not provide in some clear manner the enhancement of radiative recombination near Au NP due to local surface plasmons and radiative annihilation of plasmons themselves as well. Though, in the case of low-energy shoulders peaking at 1.6 – 1.8 eV, these mechanisms cannot be excluded. In the case of energies lower than 2.06 eV, the contribution of interband transitions to the imaginary part of gold dielectric permittivity is small. Therefore, it seems to have a low probability that the low-energy PL shoulders with peaks at 1.6 – 1.8 eV could be related with interband transitions in gold. Just opposite, it seems grounded that the PL band with its peak close to 2.4 eV is caused by radiative recombination of *sp*-electrons and *d*-holes in gold.

The fact that in Al_2O_3 films with Au NP PL disappears at the annealing temperature 800 °C and local defects of the matrix are not annealed possibly indicates that excited charge carriers escape from these defects and are scattered by large Au NP. The observed correlated dependences of the PL intensity and relaxation times on conditions providing formation of films with Au NP show that the PL efficiency is largely determined by the degree of damping the radiationless recombination channel. It is assumed that the charge carriers excited in Au NP take

part in two competitive processes: (i) radiative recombination in the same NP, (ii) escape from one Au NP and scattering on another NP. The observed non-monotonic dependences of the PL efficiency on sizes of Au NP, availability of their optimal dimensions from the viewpoint of PL intensity, on the one hand, confirms competition between these processes, and, on the other hand, compels to assume a dependence of the radiative process rate in Au NP on their sizes, shape, and properties of dielectric surrounding.

4. Conclusions

1. Obtained in this work are photoluminescent porous composite films containing gold nanoparticles in Al_2O_3 matrix by the method of one-stage pulse laser deposition using the backward particle flow from erosion torch.

2. When measuring the time-resolved photoluminescence spectra, we observed radiation within the range 1.4 – 3.2 eV with PL relaxation times lying in the range 250 ns – 5 μs.

3. We observed correlated dependences of the PL intensity and relaxation time as well as their non-monotonic dependences on the gold concentration in the target and energy density of target irradiation.

4. It is assumed that the nature of the PL band at 2.2 – 2.4 eV with relaxation times of several microseconds is related with radiative recombination of electrons and holes in Au NP. In Al_2O_3 films, the high-energy PL band at 2.9 eV with its more low-energy shoulder is related with emission of local centers in this matrix itself.

References

1. A. Mooradian, Photoluminescence of metals // *Phys. Rev. Lett*. **22**, p. 185-187 (1969).
2. G.T. Boyd, Z.H. Yu, and Y.R. Shen, Photoinduced luminescence from the noble metal and its enhancement on roughened surfaces // *Phys. Rev. B* **33**, p. 7923-7936 (1986).
3. J.P. Wilcoxon, J.E. Martin, F. Parsapour, B. Wiedenman, and D.F. Kelley, Photoluminescence from nanosize gold clusters // *J. Chem. Phys*. **108**, p. 9137-9143 (1998).
4. M.B. Mohamed, V. Volkov, S. Link, and M.A. El-Sayed, The lightning gold nanorods: fluorescence enhancement of over a million compared to the gold metal // *Chem. Phys. Lett*. **317**, p. 517-523 (2000).
5. L. Khriachtchev, L. Heikkilä, and T. Kuusela, Red photoluminescence of gold island films // *Appl. Phys. Lett*. **78**, p. 1994-1996 (2001).
6. S. Dhara, S. Chandra, P. Magudapathy, S. Kalavathi, B.K. Panigrahi, K.G.M. Nair, V.S. Sastry, C.W. Hsu, C.T. Wu, K.H. Chen, and L.C. Chen, Blue luminescence of Au nanoclusters embedded in silica matrix // *J. Chem. Phys*. **121**, p. 12595-12599 (2004).
7. T.P. Gigioni, R.L. Whetten, and Ö. Dag, Near-infrared luminescence from small gold nanocrystals // *J. Phys. Chem. B* **104**, p. 6983-6986 (2000).
8. H. Liao, W. Wen, K.L. Wong, Photoluminescence from Au nanoparticles embedded in Au:oxide composite films // *JOSA B* **23**(12), p. 2518-2521(2006).
9. G. Zhu, V.I. Gavrilenko, M.A. Noginov, Emission of Au nanoparticles with and without rhodamine 6G dye // *J. Chem. Phys*. **127**, 104503-104511 (2007).
10. E. Dulkeith, T. Niedereichholz, T.A. Klar, Plasmon emission in photoexcited gold nanoparticles // *Phys. Rev. B* **70**, 205424(4) (2004).
11. M. Eichelbaum, B.E. Schmidt, H. Ibrahim, K. Rademann, Three-photon-induced luminescence of gold nanoparticles embedded in and located on the surface of glassy nanolayers // *Nanotechnology* **18**, 355702(8) (2007).
12. C.L. Yuan, P.S. Lee, S.L. Ye, Formation, photoluminescence and charge storage characteristics of Au nanocrystals embedded in amorphous Al_2O_3 matrix // *EPL* **80**, 67003(4) (2007).
13. A.V. Kabashin, M. Meunier, Laser ablation-based synthesis of nanomaterials, In: *Recent Advances in Laser Processing of Materials*, Ed. by J. Perriere, E. Millon and E. Fogarassy. Elseveir Ltd, 2006.
14. V.S. Kortov, A.Ye. Yermakov, A.F. Zatsepin, M.A. Uimin, S.V. Nikiforov, A.A. Mysik, V.S. Gaviko, Peculiarities of luminescent properties of nanostructurized aluminum oxide // *Fizika i tekhnika poluprovodnikov* **50**(5), p. 916-920 (2008) (in Russian).
15. F.F. Komarov, N.I. Mukhurov, A.V. Mudryi, L.A. Vlasukova, A.V. Ivaniukovich, Luminescence of nano-porous aluminum oxide, In: *The Second All-Russian Conference for Nanomaterials – NANO 2007*, 13-16 March, 2007, Novosibirsk, p. 171 (in Russian).
16. D.I. Tetel'baum, A.N. Mikhailov, A.I. Belov, A.V. Yershov, Ye.A. Pitirimova, S.M. Plankina, V.N. Smirnov, A.I. Koval'ov, K. Turan, S. Verci, T.G. Finstad, S. Foss, Properties of nanostructures prepared by ion implantation of silicon into sapphire and amorphous films of aluminum oxide // *Fizika i tekhnika poluprovodnikov* **51**(2), p. 385-392 (2009) (in Russian).